

## Monitoring shoreline changes in the northern Suez Canal Zone using remote sensing and GIS applications

Ibrahim Abdel Salam A. Mohsen<sup>1</sup>, Mahmoud H. Bekiet<sup>1</sup>, Mostafa AbuBakr<sup>1,2</sup>, Atef M. Abu Khatita<sup>1,3</sup>

<sup>1</sup> Geology Department, Faculty of Science, Al-Azhar University, Cairo, Egypt.

<sup>2</sup> Center for Remote Sensing (CRS), Boston University, Boston, MA, USA.

<sup>3</sup> Geology department, College of Science, Tiabah University, Saudi Arabia.

**ABSTRACT:** The land-water boundary known as the shoreline is the area most conducive to development. Due to both natural and human influences, these areas are highly variable. To study the coastline morphology, the coastal region of the northern Suez Canal is chosen. Shoreline retreat is extracted, monitored, measured, and interpreted using GIS and remote sensing techniques. Three zones made up the area under investigation. The shoreline studying and monitoring showed that zone 1, Suffering from erosion rates was found on the coast of El-Tina plain (-17.2 to -11.9 m/year). Converted Eastward to accretion at rates reached +19.7 m/year. While over zone II, the results show that the investigated zone suffer from continuous regression (-0.82 to -5.690 m/year) and in Zone III, the results show that the investigated zone suffered from regression in the western side by rates reached -8.52 m/year and accretion at rates reached to +13.7 m/year. Prediction of shoreline position in years (2030, 2040 and 2050) is implemented based on the rates of changes.

**KEYWORDS:** Shoreline Retreat, Costal zones, Shoreline prediction

Date of Submission: 28-12-2022

Date of acceptance: 13-02-2023

### I. INTRODUCTION

Coastal zones are very changeable environments that experienced many natural and anthropogenic processes. The natural dynamic interaction between the water and the land such as waves, storms, tides, currents and winds cause continuous coastal changes over space and time. Not only nature affects the coasts but also human activities play a vital role in that concern. As most of the world's population resides in such zones, coastal areas are suffering from humans' activities. More than 80% of coasts throughout the world are exposed to retreat at annual rates ranging from 1.0 cm to 30 m (Appeaning Addo et al., 2008). The destructive coastal geological process known as coastal erosion occurs everywhere in the world. (Yining et al., 2022).

The most fluctuating area in the region of the coast is the boundary line between land and water (shoreline), which are very complicated changeable geomorphic systems (Ghoneim et al., 2015). They mentioned that the shorelines response to changes ranging from small, intermediate and large scale events. Through the small event, waves, storms winds and tides are the main factor in that changes, while the intermediate scales, shoreline changes are complicated and mainly connected to population activities (Del Río et al., 2013), but on the other hand, the large scale events, costal dynamics belonging to major events associated with climate change and land tectonics activities causing land subsidence and subsequently coasts submerging (Cowell & Thom, 1994; Del Río et al., 2013; Ghoneim et al., 2015). That intermediate term of changing occurred over decades and become in the scope of interest. Tracking the position changes of shoreline throughout the time is essential item to coastal managers (Council, 1990; Douglas, B.C. and Crowell, 2000).

Analysis of coastal zones is very important not only for coastal scientists and managers, but also, decision makers are interested in that purpose. For coastal management, it is necessary to have knowledge of where the shoreline is at the present, where it has been in the past and building models to predict where it will be found in the future. The shoreline displacement analysis has applications in many fields such as development planning, hazard zoning, erosion-accretion studies and prediction of coastal morpho-dynamics (Aedla et al., 2015). Traditional ground survey techniques are a non-economic and time-consuming approach. Over recent years, remote sensing and geographic information system (GIS) environments provide improved capabilities to study shoreline

deflections. It can handle the accurate geographic position of the coastline and calculate the changes over the coastal zones. GIS software such as Digital Shoreline Analysis System (DSAS) are widely used for that target (Aedla et al., 2015; Basu and Mitra, 2016; Cenci et al., 2018; El Sharnouby and El Alfy, 2015). With the help of historical data, many statistics have been assessed for shoreline projection in the future (Nassar et al., 2018). The most widespread and utilized models for that purpose includes End Point Rate (EPR) model, Average of Rates (AOR), Least Median of Squares (LMS), Linear Regression Rate (LRR) and Jackknife model (JK) (Burgess et al., 2004; Moran, 2003).

Several studies investigated shoreline position over space and time such as (Aedla et al., 2015; Appeaning Addo et al., 2008; Basu and Mitra, 2016; Bengali, 2018; Cenci et al., 2018; Douglas, B.C. and Crowell, 2000; Makota et al., 2004; Xu, 2018).

Recently the Egyptian government looking forward to develop the Suez Canal District. In order to accommodate the independent passage of ships traveling in opposing directions, a new 72-kilometer-long second shipping lane was dug within the 164-kilometer-long canal as part of the development planning process. Furthermore, the government aspires to convert the area into a top-notch global transportation hub and industrial processing hub that services the markets of the American, Asian, and European continents. Consequently, this will encourage and promote the Egyptian people's economic development and prosperity. However, with the expected increase in transiting vessels and industrial activity, the environmental impact of this growth needs to be accurately assessed and managed. There for, the present study aims to utilize series of Landsat data over 30 years-time-span to monitor assess, track and predict the shoreline displacement over the investigated area.

### Study area

Suez Canal is an artificial waterway located in the northeastern part of Egypt connecting the Gulf of Suez and the Mediterranean Sea. It is surrounded northwards by the Mediterranean Sea, eastwards by the Sinai Peninsula, southwards by the Gulf of Suez and the Red sea and westwards by the Nile Delta. Suez Canal Zone is generally dominated by water bodies and lowlands covered by soft gravels and friable sandstone with silt and clay intercalations. The Suez Canal sedimentary covers belong to ages from cretaceous to recent (El Shazly et al., 1975). In the northern part, most of the sediments are related to the Pleistocene and Recent (Gaber M., 1993). The Pelusium shear system (NE to SW) is the main structural feature across the Suez Canal zone which is derived mainly from the shoulder cliff of the Gulf of Suez with downthrown side toward the Mediterranean Sea (Gamal, 2013). In this thesis we divided the investigated area into three zones as shown in (Fig. 1). Zone I extends from the entrance of the Canal eastward to the beginning of El-Bardawile Lake. Zone II extends over Port Fouad city and the maritime. Zone III extends over Port Said city westward of the Suez Canal.

## II. Materials and Methods

The location of the coastline in the area under investigation was determined using multi-temporal satellite data from the Landsat series TM, ETM, and OLI/TIRS during a 30-year period. Between 1987 and 2017, the images were regularly downloaded from the USGS Global Visualization Viewer (GloVis, <http://glovis.usgs.gov/>) (Table 1). In order to prevent clouds, the summer season was chosen for the data. The Landsat scenes used for this project are Level 1 Terrain corrected (L1T) products, which are radiometrically and geometrically corrected data for the terrain.

### 2.1. Shoreline extraction from satellite imagery

The significant absorption of water in the near-infrared and mid-infrared regions of the electromagnetic spectrum is the primary basis for the coastline extraction in this work. Therefore, signal near-infrared band segmentation thresholding was carried out using Environment for Visualizing Images (ENVI) software version 5.3, where the reflectance of water close to zero. Because the Scan Line Corrector failed (SLC-off) in May 2003, Simple gap-filling practice were implemented on the Landsat 7 (ETM+) image to match the missing pixel data (Fig. 2). The mentioned thresholding technique, making it easy to distinguish land from water and binary image can be gained. Hence the chosen method was applied to four Landsat images (Table 1) and generated 4 binary images (Fig. 3). All of the binary raster converted to vector polygons data set using ArcGIS software (version 10.4). Every polygon transformed into line shape file and extracted the shoreline. All the shorelines were combined in a single shape file as shown in (Fig. 4). All processing and results interpreting procedures were performed in the laboratory of remote sensing and GIS, Al-Azhar University (Fig. 5).

### 2.2. Shoreline change rate and future prediction

In recent, GIS environments have the ability to study shoreline morphology deflections. The shoreline changes for the investigated area over 30 years were calculated using the Digital Shoreline Analysis System (DSAS) Version 4.4. DSAS is a software Published by the United States Geological Survey (USGS). It works as an add-on extension to Environmental Systems Research Institute (ESRI) ArcGIS software that allows to calculate shoreline rate of change statistics from multiple historic shoreline positions (Thieler et al., 2012).

Firstly, baseline which acts as a reference for the remote sensing derived shorelines were created. A total number of 754 transects for Zone I, 79 for Zone II and 589 for Zone III with 50-meter intervals were generated perpendicular to the reference baseline. In order to verify the authenticity of the Landsat-derived shorelines for coastal analysis, the extracted shorelines were overlaid on Google Earth.

To compute change statistics over the examined area, linear regression rate (LRR) and end point rate (EPR) are utilized. By dividing the distance between the oldest and most recent shorelines by the amount of time they have been there, the EPR is computed. By fitting a least-squares regression line to all shoreline locations for a specific transect, the LRR of change statistic can be calculated (Thieler et al., 2012). The End Point Rate (EPR) model was used to forecast future positions of the shoreline along the study area.

### III. RESULTS And DISCUSSIONS

Over a thirty-year period, shoreline change detection has been observed along the Suez Canal Zone's northern coastal section (1987–2017). Multi-spectral series of Landsat imageries were utilized. Segmentation thresholding for signals near-infrared bands has been used to extract shoreline positions. The research area's change rate was detected using the end point rate module. For accurate erosion and accretion tracing the study area has been classified into three zones. Over zone I, the results show that change rates varied over the investigated zone. Highly erosion rates were found in on the coast of El-Tina plain (-17.2 to -11.9 m/year) (Fig. 6). The erosion has been decreased eastward and converted to accretion at rates reached +19.7 m/year. Over zone II, the findings indicate that the examined zone continues to experience coastline regression at rates between (-0.82 and -5.690 m/year) (Fig. 7). While in Zone III, the results show that the investigated zone suffered from regression in the western side by rates reached to -8.52 m/year and accretion at rates reached to +13.7 m/year (Fig. 8). These results lead to figure the coast environment over the northern part of the Suez Canal coast. This regression in the shoreline may be related to some natural and human activity factors. Sea Level rising resulted from climate change and natural subsidence have playing important role in that propose. By 2100, the sea level would increase by 0.8 to 1.2 meters because of climate change, according to the Intergovernmental Panel on Climate Change (IPCC). (Gaber et al., 2014) stated that the total land subsidence over the study area was found to be 17 mm during the period from 2007 to 2010. On the other hand, the shipping and industrial activities made sense in the shoreline retreat. The ship traffics may generate an additional current beside the natural current which can increase the submerged areas. The results show that Zone two of the shoreline is more vulnerable to coastal erosion as it has a continuous retreat and the position of that Zone.

Zone two is the port Fouad coastline, which is regarded as a crucial component in the global transportation sector due to its location at the waterway's entrance to the Suez Canal. There is a danger of flooding in the area due to the zone's erosion rate, which ranges from 0.8 to 5.6 meters per year. So, three temporal scenarios were used to detect the spatial extent of the retreat in the assumption of the rates still constant, the positions of the three temporal scenarios are shown in (Fig. 9). As the Egyptian as the decision-makers is very interested in this area, there is an urgent need to take further measures against this retreat in order to protect this important zone.

### IV. Conclusion

The analysis of the results suggests that the remote sensing data along with geographic information systems have the ability to monitor and assessing shoreline retreat. The long-term of shoreline change is extensively investigated over the coastal area of the northern part of the Suez Canal Zone over 30 years (1987- 2017). Shoreline positions are extracted over the study area in 1987, 1997, 2007 and 2017 respectively. Digital Shoreline Analysis System (DSAS) Version 4.4. DSAS were used to calculate shoreline rate-of-change statistics from the extracted positions. The EPR module was used to make three scenarios of the future shoreline position. The results show that the coastal area of the northern part of the Suez Canal is subjected to coastal erosion and needs artificial protection especially in the area of zone two.

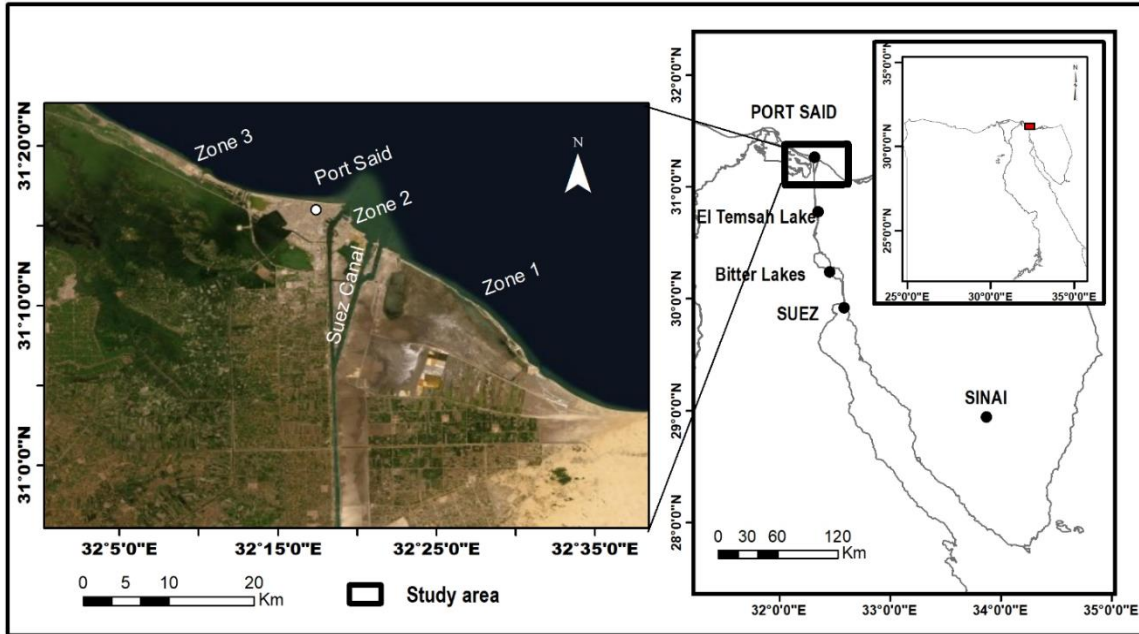


Fig. 1. Location map indicating the three zones of the area under investigation.

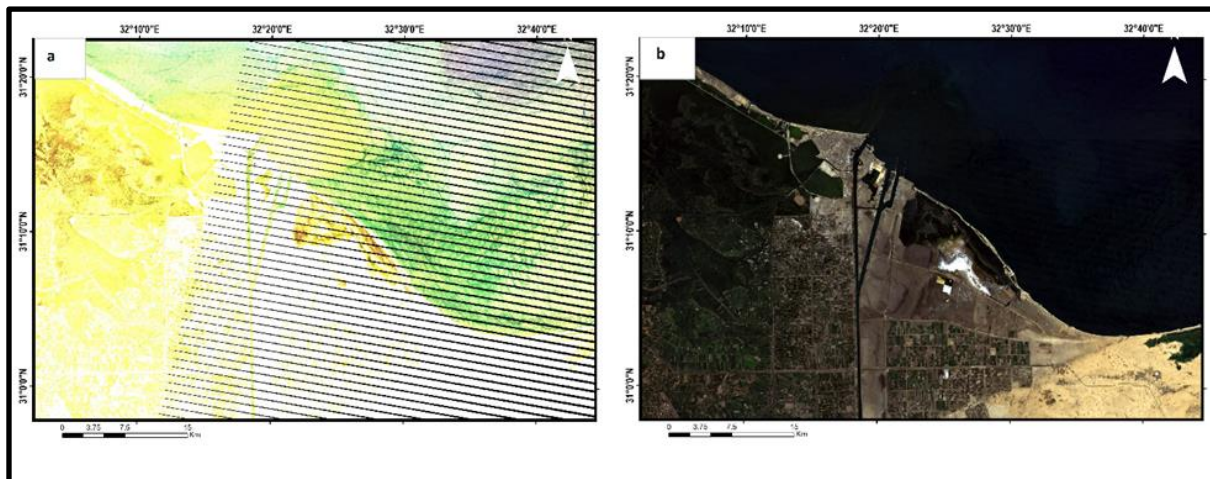


Fig. 2. Gap filling Landsat 7 SLC off data using ENVI. (a) Post SLC failure (b) after SLC correction.



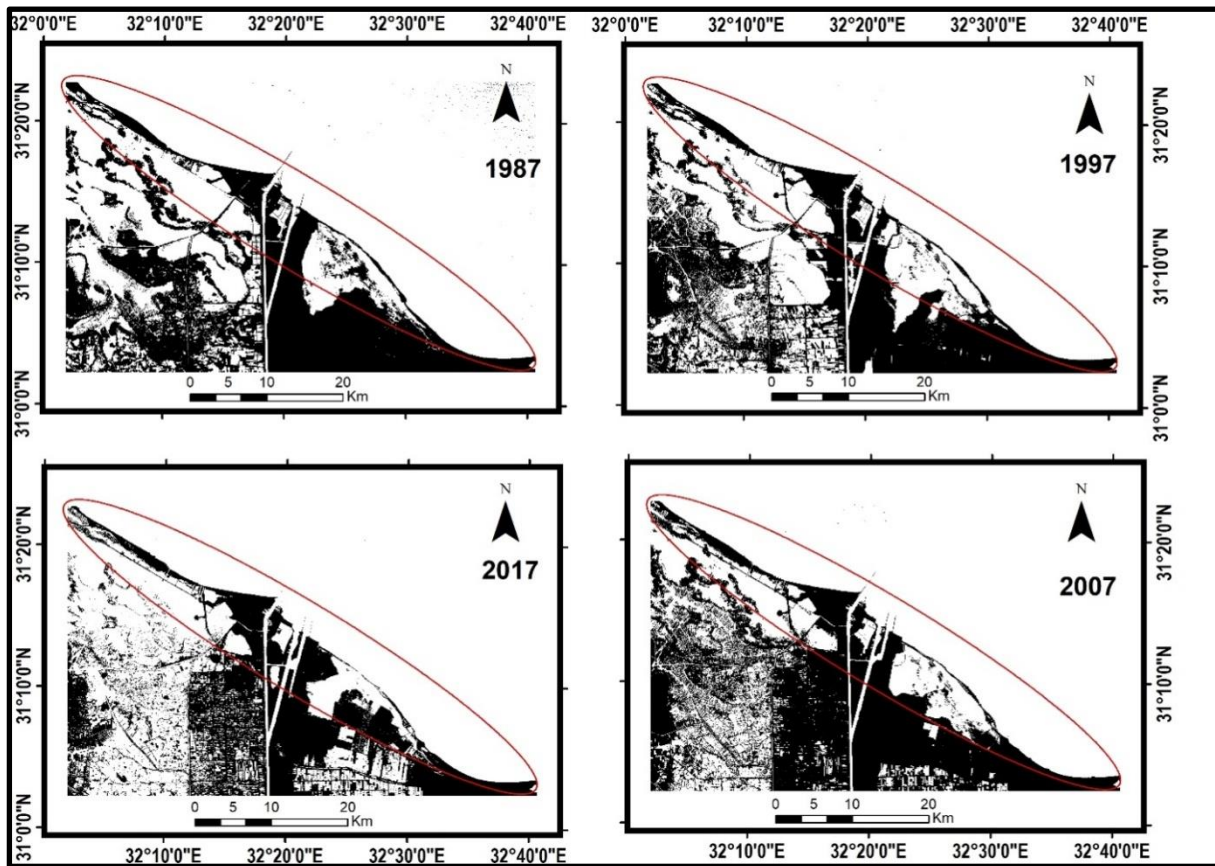


Fig. 3. Four binary images resulted from segmentation thresholding for 1987, 1997, 2007 and 2017 dates respectively.

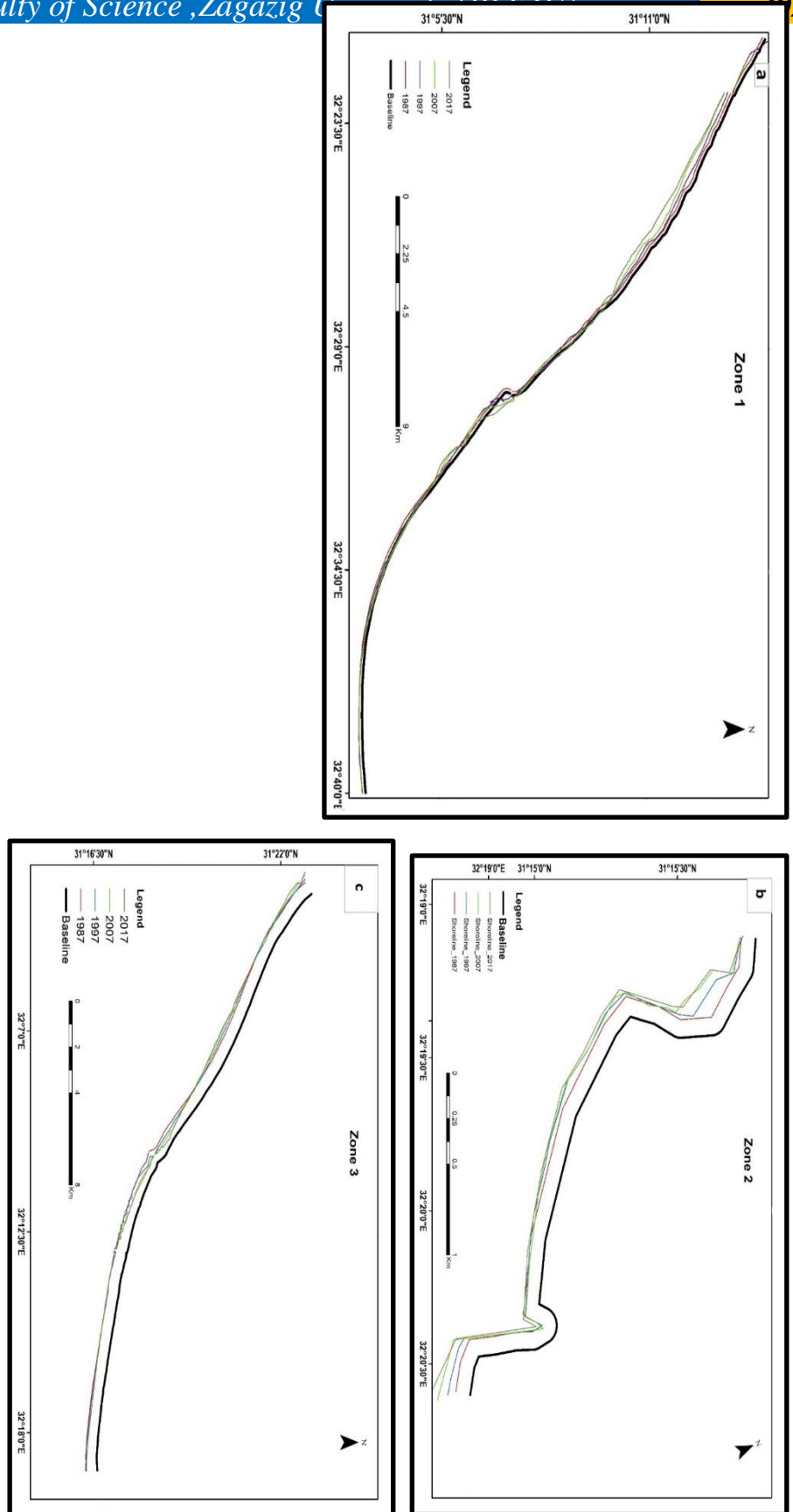


Fig. 4. The extracted shorelines are collected in single shape file for zones 1, 2 and 3 respectively.

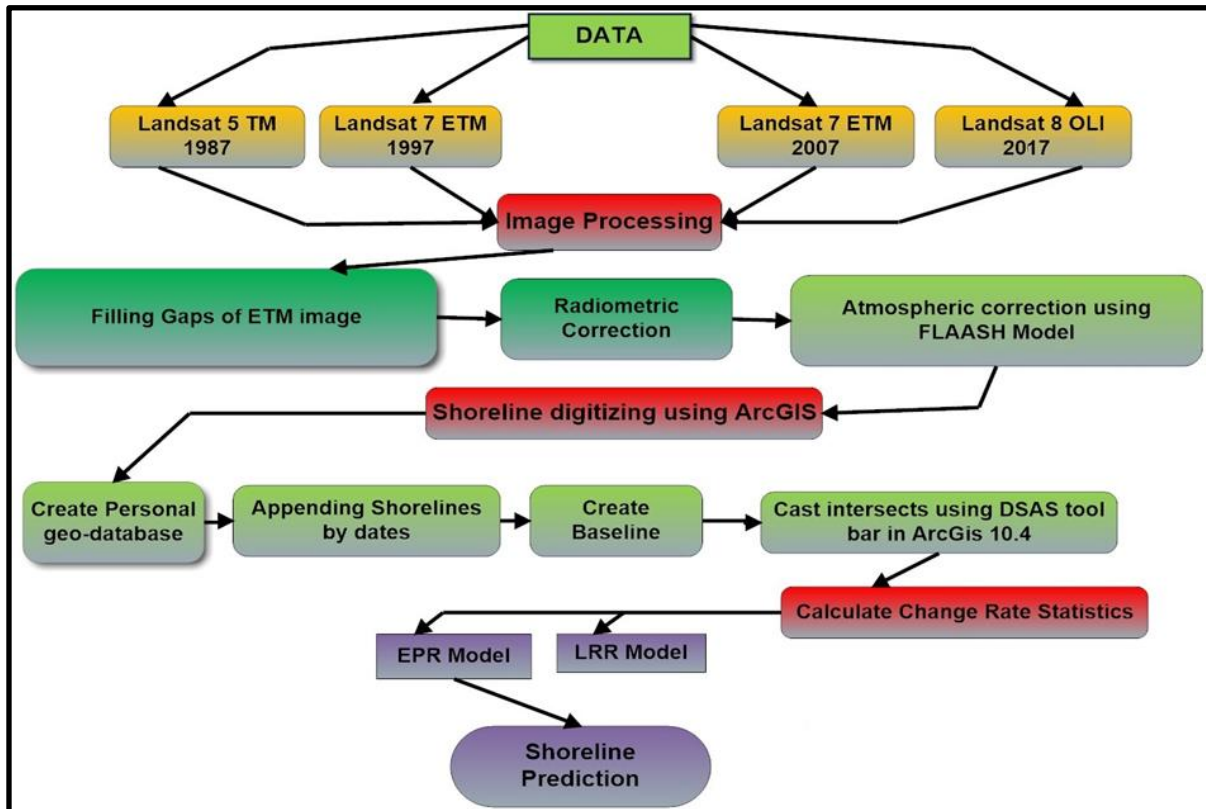


Fig. 5. Flow chart illustrating procedures of processing and results.

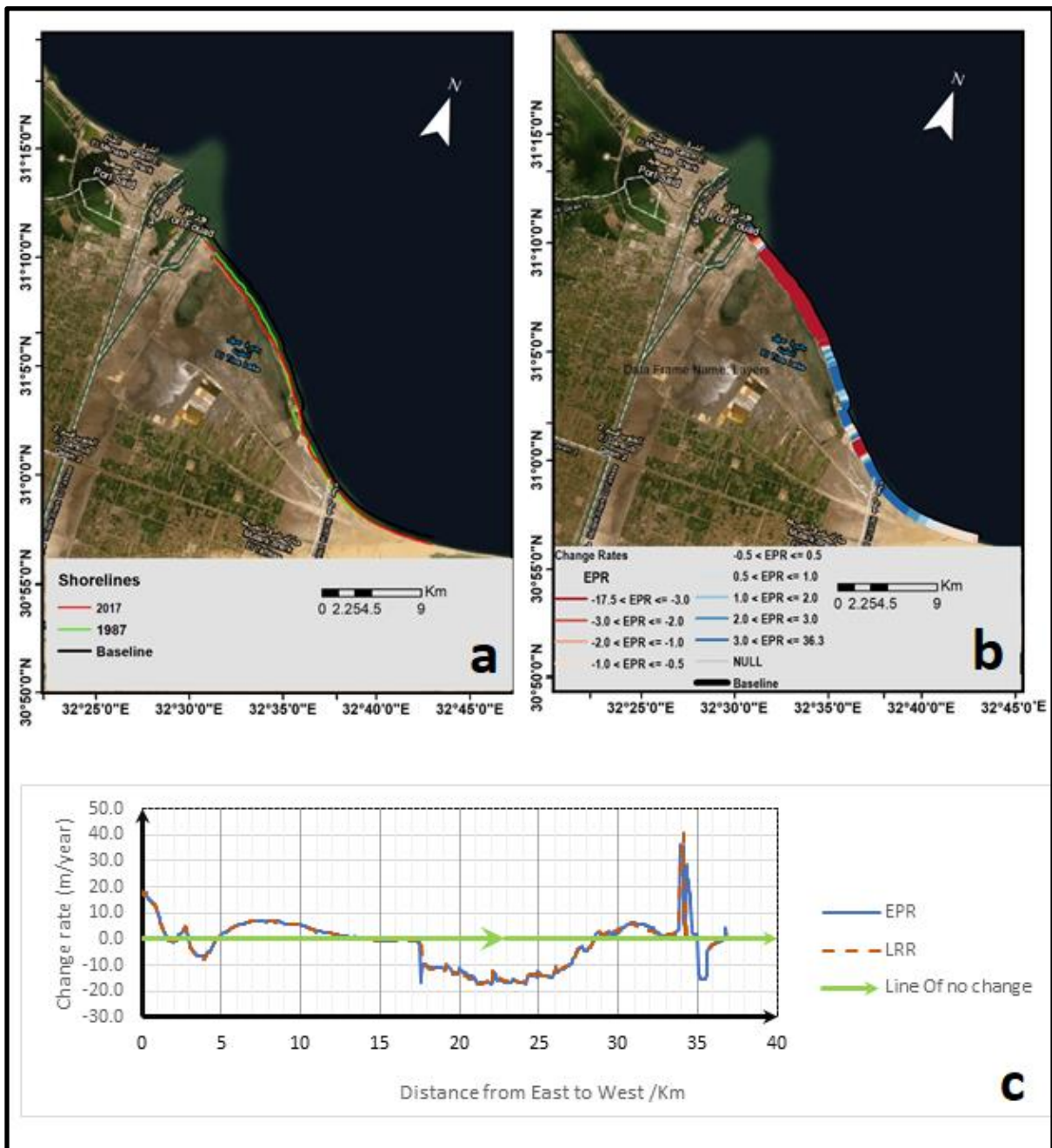


Figure 6: Shore line change rates on Zone 1, (a) Extracted shorelines for years 2017 and 1987, (b) Shore line change rates, (c) Change rates via distance from east to west.



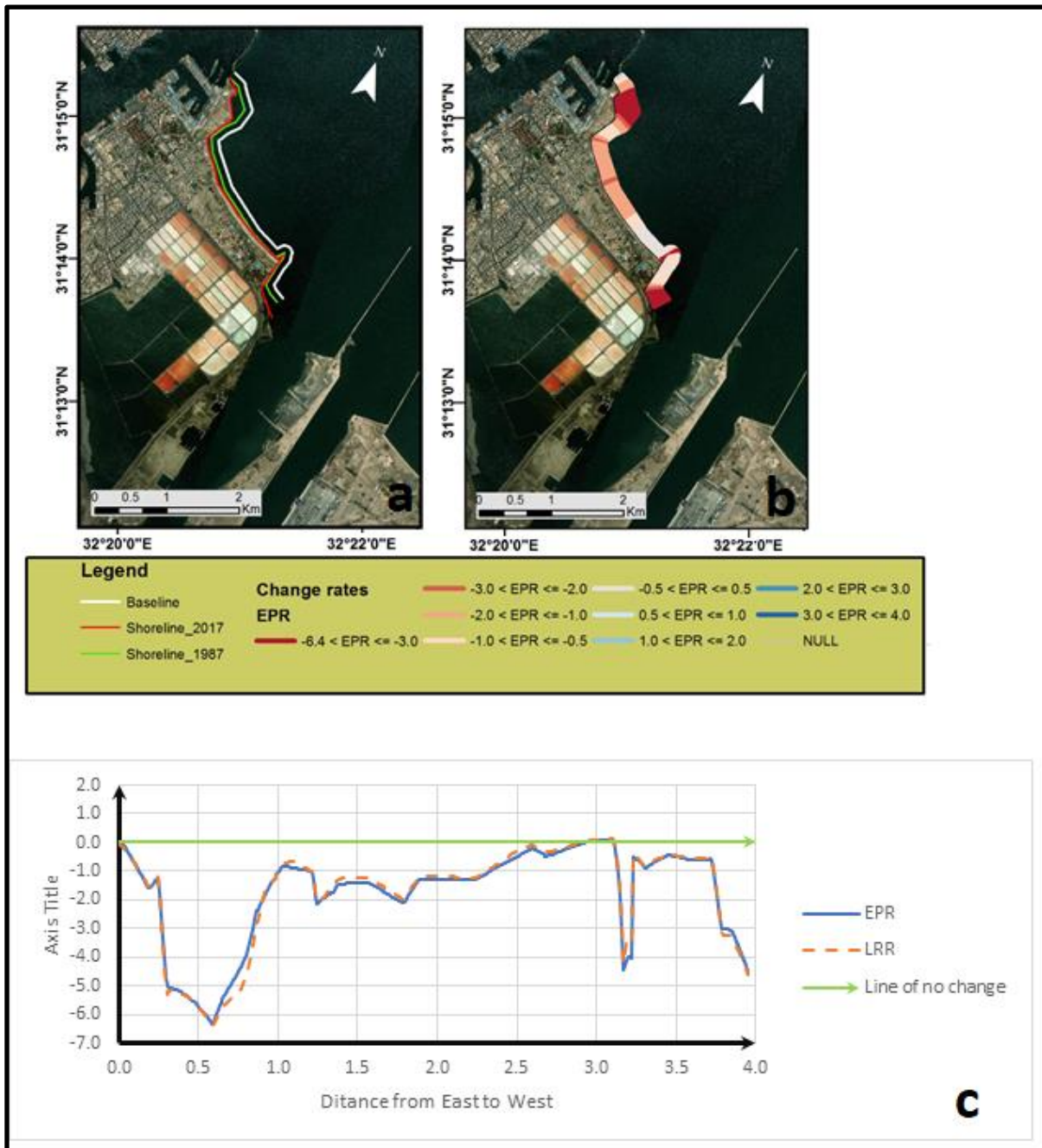


Figure 7: Shore line change rates on Zone 2, (a) Extracted shorelines for years 2017 and 1987, (b) Shore line change rates, (c) Change rates via distance from east to west.

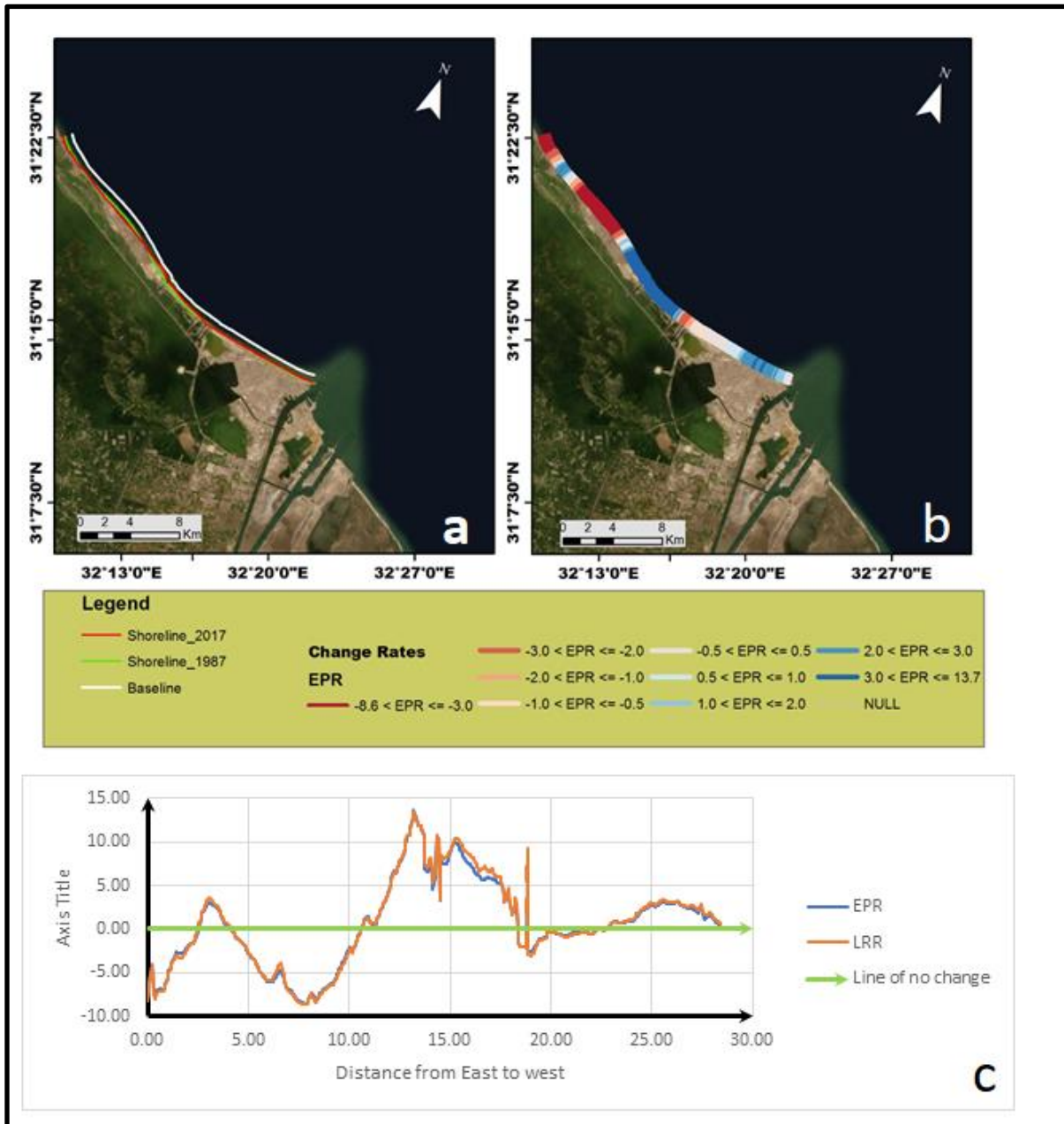


Fig. 8: Shore line change rates on Zone 3, (a) Extracted shorelines for years 2017 and 1987, (b) Shore line change rates, (c) Change rates via distance from east to west.

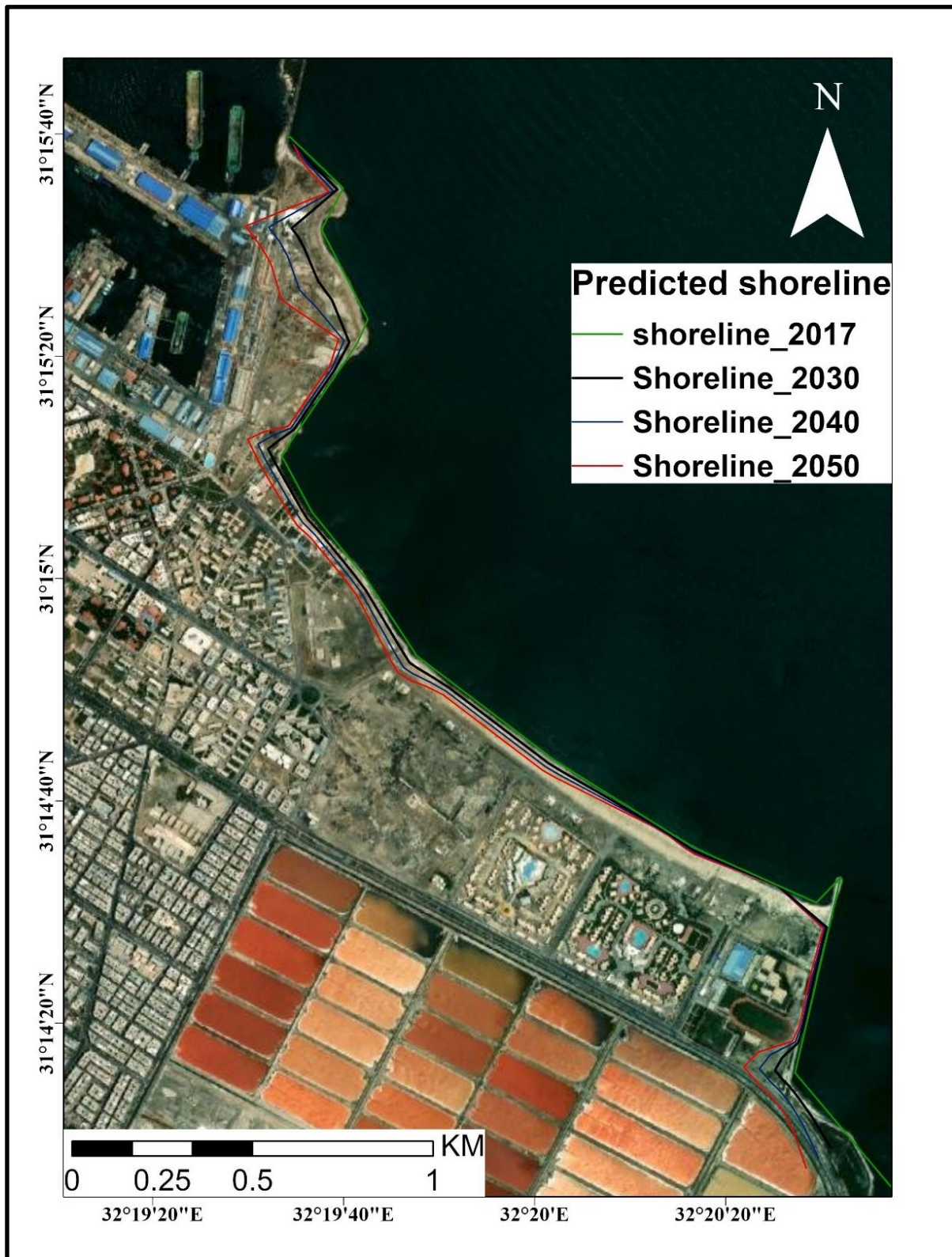


Figure 9 shows a projection of future shorelines over Zone II. The green line shows where the shoreline is in 2017; the black line shows where it will be in 2030; the blue line shows where it will be in 2040; and the red line shows where it will be in 2050.



Table 1: details of Landsat data

Acquisition date	Sensor type	Path/Raw	Spatial resolution
27/07/1987	Landsat 5 – TM	176/38	30 m
22/07/1997	Landsat 5 – TM		30 m
27/08/2007	Landsat 7 – ETM+		30 m
13/07/2017	Landsat 8 -OLI/TIRS		30 m

## REFERENCES

- Aedla, R., Dwarakish, G. S., & Reddy, D. V. (2015).** Automatic Shoreline Detection and Change Detection Analysis of Netravati-Gurpur River mouth Using Histogram Equalization and Adaptive Thresholding Techniques. *Aquatic Procedia*, 4(Icwrcoe), 563–570. <https://doi.org/10.1016/j.aqpro.2015.02.073>.
- Appeaning Addo, K., Walkden, M., & Mills, J. P. (2008).** Detection, measurement and prediction of shoreline recession in Accra, Ghana. *ISPRS Journal of Photogrammetry and Remote Sensing*, 63(5), 543–558. <https://doi.org/10.1016/j.isprsjprs.2008.04.001>
- Basu, A., & Mitra, D. (2016).** Shoreline change detection using geospatial technologies : A case study on a part of West Bengal Coast, Bay of Bengal. 1(July).
- Bengal, W. (2018).** Shoreline change detection using Remote Sensing in the Bakkhali Coastal Region, West Bengal, India. August.
- Burgess, K., Jay, H., & Hosking, A. (2004).** Future coast: Predicting the future coastal evolution of England and Wales. *Journal of Coastal Conservation*, 10(1–2), 65–71. [https://doi.org/10.1652/1400-0350\(2004\)010\[0065:FPTFCE\]2.0.CO;2](https://doi.org/10.1652/1400-0350(2004)010[0065:FPTFCE]2.0.CO;2)
- Cenci, L., Disperati, L., Persichillo, M. G., Oliveira, E. R., Alves, F. L., & Phillips, M. (2018).** Integrating remote sensing and GIS techniques for monitoring and modeling shoreline evolution to support coastal risk management. *GIScience and Remote Sensing*, 55(3), 355–375. <https://doi.org/10.1080/15481603.2017.1376370>
- Council, N. R. (1990).** Managing Coastal Erosion. NATIONAL ACADEMY PRESS Washington. <https://doi.org/10.17226/1446>
- Cowell, P. J., & Thom, B. G. (1994).** Morphodynamics of coastal evolution. In: Carter, R.W.G., Woodroffe, C.D. (Eds.), *Coastal Evolution: Late Quaternary Shoreline Morphodynamics*. In Cambridge University Press (Issue Cambridge, pp. 33–86).
- Darwish, K., Smith, S. E., Torab, M., Monsef, H., & Hussein, O. (2017).** Geomorphological Changes along the Nile Delta Coastline between 1945 and 2015 Detected Using Satellite Remote Sensing and GIS. *Journal of Coastal Research*, 33(4), 786–794. <https://doi.org/10.2112/JCOASTRES-D-16-00056.1>
- Del Río, L., Gracia, F. J., & Benavente, J. (2013).** Shoreline change patterns in sandy coasts. A case study in SW Spain. *Geomorphology*, 196, 252–266. <https://doi.org/10.1016/j.geomorph.2012.07.027>
- Douglas, B.C. and Crowell, M. (2000).** Long-term shoreline position prediction and errorpropagation. *Journal of Coastal Research*, 16(1), 145–152.
- El Sharnouby, B. A., & El Alfy, K. S. (2015).** Coastal Changes along Gamasa Beach, Egypt. *Journal of Coastal Zone Management*, 18(1), 1–11. <https://doi.org/10.1016/j.ijbiomac.2008.03.002>
- EL-SHAZLY E., M. ABDEL HADY, A. SALMAN, W. MESHERF, M. MORSY, M. EL RAKAIBY, I. EL\_AASSY, A. KAMEL, A. AMMAR, AND M. MELEIK. (1975).** Geological and geophysical investigations of the Suez Canal zone, Remote sensing research project academy of scientific research and technology, Cairo, Egypt.
- Gaber, A., Darwish, N., Sultan, Y. M., Arafat, S. M., & Koch, M. (2014).** Monitoring Building Stability in Port-Said City, Egypt Using Differential SAR Interferometry. *International Journal of Environment*, 3.
- Gamal, M. A. (2013).** Truthfulness of the Existence of the Pelusium Megashear Fault System, East of Cairo, Egypt. *International Journal of Geosciences*, 04(01), 212–227. <https://doi.org/10.4236/ijg.2013.4101>
- Ghoneim, E., Mashaly, J., Gamble, D., Halls, J., & Abubakr, M. (2015).** Nile Delta exhibited a spatial reversal in the rates of shoreline retreat on the Rosetta promontory comparing pre- and post-beach protection Geomorphology Nile Delta exhibited a spatial reversal in the rates of shoreline retreat on the Rosetta promontory. *Geomorphology*, 228(January), 1–14. <https://doi.org/10.1016/j.geomorph.2014.08.021>
- M. Gaber (1993).** Geology of the northern reaches of the Suez Canal area and its surroundings. *Annals of Geological Survey of Egypt*, v, xix (1993) p 513-523.
- Makota, V., Sallema, R., & Mahika, C. (2004).** Monitoring Shoreline Change using Remote Sensing and GIS : A Case Study of Kunduchi Area, Tanzania. *Western Indian Ocean J. Mar. Sci*, 3(1), 1–10.
- Moran, C. A. A. (2003).** SPATIO-TEMPORAL ANALYSIS OF TEXAS SHORELINE CHANGES USING GIS TECHNIQUE (Issue December). <https://doi.org/10.16309/j.cnki.issn.1007-1776.2003.03.004>

- Nassar, K., Fath, H., Mahmud, W. E., Masria, A., Nadaoka, K., & Negm, A. (2018).** Automatic detection of shoreline change: case of North Sinai coast, Egypt. *Journal of Coastal Conservation*, 1–27. <https://doi.org/10.1007/s11852-018-0613-1>
- Thieler, E. R., Himmelstoss, E. A., Zichichi, J. L., & Ergul, A. (2012).** Digital Shoreline Analysis System (DSAS) version 4.0—An ArcGIS extension for calculating shoreline change (ver. 4.3, April 2012): U.S. Geological Survey Open-File Report 2008-1278.
- USGS Global Visualization Viewer (GloVis). (n.d.).** Accessing remote sensing data. <https://glovis.usgs.gov/>
- Xu, N. (2018).** Detecting coastline change with all available Landsat data over 1986-2015: A case study for the state of Texas, USA. *Atmosphere*, 9(3). <https://doi.org/10.3390/atmos9030107>
- Zhou, Y., Tian, S., Wang, H., Chang, C., Gao, Y., Zhang, B., & Wang, X. (2022).** Coastal change detection along the Fire Island, US under the impact of Hurricane Sandy based on Lidar data. *ISPRS Annals of the Photogrammetry, Remote Sensing and Spatial Information Sciences*, 3, 569-575.